



Fermi National Accelerator Laboratory

FERMILAB-Pub-99/162-E

CDF

Luminosity Monitoring and Measurement at CDF

D. Cronin-Hennessy, A. Beretvas and P.F. Derwent
For the CDF Collaboration

*Fermi National Accelerator Laboratory
P.O. Box 500, Batavia, Illinois 60510*

June 1999

Submitted to *Nuclear Instruments and Methods in Physics Research*

Disclaimer

This report was prepared as an account of work sponsored by an agency of the United States Government. Neither the United States Government nor any agency thereof, nor any of their employees, makes any warranty, expressed or implied, or assumes any legal liability or responsibility for the accuracy, completeness, or usefulness of any information, apparatus, product, or process disclosed, or represents that its use would not infringe privately owned rights. Reference herein to any specific commercial product, process, or service by trade name, trademark, manufacturer, or otherwise, does not necessarily constitute or imply its endorsement, recommendation, or favoring by the United States Government or any agency thereof. The views and opinions of authors expressed herein do not necessarily state or reflect those of the United States Government or any agency thereof.

Distribution

Approved for public release; further dissemination unlimited.

Copyright Notification

This manuscript has been authored by Universities Research Association, Inc. under contract No. DE-AC02-76CHO3000 with the U.S. Department of Energy. The United States Government and the publisher, by accepting the article for publication, acknowledges that the United States Government retains a nonexclusive, paid-up, irrevocable, worldwide license to publish or reproduce the published form of this manuscript, or allow others to do so, for United States Government Purposes.

Luminosity Monitoring and Measurement at CDF

D. Cronin-Hennessy^{a*}, A. Beretvas^b, P. F. Derwent^b

^aDuke University,
Durham, North Carolina 27708, USA

^bFermi National Accelerator Laboratory
Batavia, Illinois 60510, US

Using two telescopes of beam-beam counters, CDF (Collider Detector at Fermilab) has measured the luminosity to an accuracy of 4.1% (3.6%) in run Ib(Ia). For run Ib (Ia) the average luminosity was $9.1(3.3) \times 10^{30} \text{ cm}^{-2}\text{sec}^{-1}$. For a typical data set the integrated luminosity was 86.47 (19.65) pb^{-1} in run Ib (Ia) resulting in a total integrated luminosity of $106.1 \pm 4.1 \text{ pb}^{-1}$. This paper shows how we have determined the accuracy of our results.

1. Introduction

In this article we present a detailed description of how the Collider Detector at Fermilab (CDF) experiment measured luminosity during Run I (1992-1996). The beam-beam counters (BBC) consisted of two sets of scintillation counters located at ± 5.82 m from the nominal interaction point [1]. These counters provided a “minimum-bias” trigger and were used as the primary luminosity monitor. The counters were arranged in a rectangle around the beam pipe [2]. There were 16 scintillation counters in each set, with two phototubes attached to each scintillator, and both an anode and an inverted dynode signal are taken from each phototube. The data acquisition system includes a set of scalers which count a combination of intime and out of time hits in the BBC, the most important of which are the intime hits for the 32 counters. The counters were at a low angle to the beam directions and they cover the angular region (measured along either the horizontal or vertical axes) from 0.32° to 4.47° (179.68° to 175.53°), corresponding to a pseudorapidity range of 3.24 to 5.90. The beam-beam counters were designed for a luminosity of $1 \times 10^{30} \text{ cm}^{-2}\text{sec}^{-1}$, but continued to work correctly at a luminosity of $1.2 \times 10^{31} \text{ cm}^{-2}\text{sec}^{-1}$.

In section 2 we give the accelerator parameters for run I, and in section 3 we describe the history of σ_{BBC} at CDF. In the next section we present the basic formulae for the luminosity calculation. Section 5 describes the multiple interaction formula. In section 6 we present the details of the luminosity calculation. Section 7 describes the uncertainty in the luminosity for run Ia. In the following sections, we present checks that give confidence in the performance of the BBC over changes in time and instantaneous rate (with luminosity varying from $2 \times 10^{30} \text{ cm}^{-2}\text{sec}^{-1}$ to $2 \times 10^{31} \text{ cm}^{-2}\text{sec}^{-1}$) during run Ib. Section 8 presents a consistency check of the luminosity using $W \rightarrow e\nu$ decays. Section 9 presents the run to run variation in the W cross section for run Ib. Section 10 presents the systematic errors due to high instantaneous luminosity (run Ib). A consistency check for the luminosity is given in Section 11. This check measures the ratio of events with one or more vertices to the number with no vertices as a function of luminosity. Section 12 describes the prescale factors and the determination of the luminosity for all triggers used in the experiment.

2. Accelerator parameters

Before explaining the beam-beam counters, we will briefly present the luminosity in terms of the

*present address: University of Rochester, Rochester, New York 14627

accelerator parameters. The luminosity for a synchrotron collider assuming head-on collisions is

$$L = \frac{3\gamma f_0 N_B N_p N_{\bar{p}} F}{\beta^* (\epsilon_p + \epsilon_{\bar{p}})} \quad (1)$$

where $\gamma = E/m$ is the relativistic energy factor, f_0 is the revolution frequency, β^* is the beta function at the low beta focus, N_B is the number of bunches, N_p ($N_{\bar{p}}$) is the number of protons (antiprotons) per bunch, ϵ_p ($\epsilon_{\bar{p}}$) is the proton (antiproton) beam emittance and F is the form factor. The form factor describes the reduction in the luminosity when the bunch length is comparable to the beta function.

At Fermilab we have had the following runs: 1985 (first collisions), 1987 (a very low luminosity run), 1988-89, run Ia (1992-1993) and run Ib (1994-1996). The accelerator parameters are given in Table 1 [3], [4]. All runs have been taken with a beam energy of 900 GeV ($\sqrt{s} = 1800$ GeV). East (west) refers to proton beam downstream (upstream) of the interaction point.

3. The history of σ_{BBC} at CDF

All cross sections at CDF are defined with respect to the coincidence rate in the two sets of BBC. Given the BBC cross section (σ_{BBC}) we only need to determine the number of BBC interactions (N_{BBC}) during the time CDF is “live” to derive a luminosity.

$$L = \frac{N_{\text{BBC}}}{\sigma_{\text{BBC}}} \quad (2)$$

A BBC interaction is defined as follows: the coincidences of an intime hit in any of the 16 counters on the east side and an intime hit in any of the 16 counters on the west side, where an intime hit is a hit in a 30 nsec gate centered on the expected arrival time.

The values we have used for σ_{BBC} are given in Table 2. The BBC cross section is related to the total cross section (σ_{total}) as follows:

$$\sigma_{\text{BBC}} = \sigma_{\text{total}} \frac{N_{\text{BBC}}}{N_{\text{inel}} + N_{\text{el}}} \quad (3)$$

where N_{inel} and N_{el} are the total number of inelastic and elastic events. Initially we used a value of

$\sigma_{\text{BBC}} = 44 \pm 6.6$ mb [5]. This value was based on using a UA4 total cross section measurement at $\sqrt{s} = 546$ GeV [6] and UA5 at $\sqrt{s} = 900$ GeV [7]. The integrated luminosity for this first run was approximately 25 nb^{-1} . Our next run in 1988-89 used a value of $\sigma_{\text{BBC}} = 46.8 \pm 3.2$ mb [8]. This method combined beam parameters and accelerator lattice information with the UA4 measurement. The UA4 experiment used trigger counters with similar geometry to our BBC. We corrected the UA4 measurement for both a different η range and radiation damage suffered by the BBC during the run. The integrated luminosity for this run was approximately 4 pb^{-1} . During this run CDF took a short dedicated run to measure the elastic [9], diffractive [10], and total cross section [11]. The total proton-antiproton cross section was measured at both $\sqrt{s} = 546$ and 1800 GeV using the luminosity independent method. The total cross section was $(1 + \rho^2)\sigma_{\text{total}}(1800) = 81.83 \pm 2.29$ mb, where ρ is the ratio of the real to imaginary part of the forward scattering amplitude. Using the total cross section and $\rho = 0.140$ [12], $\sigma_{\text{total}} = 80.26 \pm 2.25$ mb. If the error on ρ (± 0.069) is included then our result is 80.26 ± 2.71 mb.

We can express the number of inelastic events as

$$N_{\text{inel}} = N_i + N_{\text{sd}} \quad (4)$$

where N_i is the number of events with a two-sided coincidence in either the BBC or forward telescopes [11], and N_{sd} is the number of events ($\times 2$) with a single \bar{p} detected in the forward magnetic spectrometer [11] coincident with hits in the opposite side BBC or forward telescope [13]. We express σ_{BBC} as

$$\sigma_{\text{BBC}} = \sigma_{\text{total}} \frac{\frac{N_{\text{BBC}}}{N_i}}{1 + \frac{N_{\text{sd}} + N_{\text{el}}}{N_i}} \quad (5)$$

The quantity N_i is a superset of N_{BBC} and includes a Monte Carlo acceptance correction of 1.2%. We find 98.7% of N_i triggered events are BBC triggered events. Therefore $N_{\text{BBC}}/N_i = 0.987/1.012 = 0.975$. The values of N_{sd} , N_{el} and N_i are 32,092, 78,691, and 208,890 respectively [11]. These numbers and their errors are given in Table 3.

Table 1
Fermilab Collider Parameters

Collider parameters	88-89 Run	Run Ia	Run Ib
N_p Proton/bunch (10^{10})	7.0	12.0	22.5
$N_{\bar{p}}$ Antiprotons/bunch (10^{10})	2.9	3.1	6.5
ϵ_p Proton emittance (π mm-mr)	25	20	22
$\epsilon_{\bar{p}}$ Antiproton emittance (π mm-mr)	18	12	14
β^* at interaction point (cm)	55	35	35
N_B Number of bunches	6	6	6
Form Factor	0.71	0.62	0.62
Beam Energy (GeV)	900	900	900
γ	959	959	959
Circumference (km)	6.28	6.28	6.28
f_0 revolution frequency (10^4 sec $^{-1}$)	4.78	4.78	4.78
Typical initial luminosity (10^{31} cm $^{-2}$ sec $^{-1}$)	0.16	0.54	1.89

Table 2
Values of σ_{BBC}

Cross Section	87 Run	88-89 Run	Run Ia	Run Ib
σ_{BBC} (mb)	44 ± 6.6	46.8 ± 3.2	51.15 ± 1.60	51.15 ± 1.60

We can rewrite Eq. 5 as

$$\sigma_{BBC} = \frac{k(\frac{N_{BBC}}{N_i})AN_i}{(A/b + N_i + N_{sd})^2} \quad (6)$$

where

$$k = \frac{16\pi(\hbar c)^2}{(1 + \rho^2)} = \frac{19.572}{(1 + \rho^2)} \text{ GeV}^2 \quad (7)$$

and $N_{el} = A/b$, where $A = dN_{el}/dt|_{t=0}$ is the number of elastic events evaluated where the four-momentum transfer squared, $-t$, equals zero and b is the logarithmic elastic slope parameter [9]. The error on σ_{BBC} is obtained from:

$$\begin{aligned} (\Delta\sigma_{BBC})^2 &= \left(\frac{\partial\sigma_{BBC}}{\partial N_i}\right)^2(\Delta N_i)^2 \\ &+ \left(\frac{\partial\sigma_{BBC}}{\partial N_{sd}}\right)^2(\Delta N_{sd})^2 \\ &+ \left(\frac{\partial\sigma_{BBC}}{\partial A}\right)^2(\Delta A)^2 \\ &+ \left(\frac{\partial\sigma_{BBC}}{\partial b}\right)^2(\Delta b)^2 \\ &+ 2 \cdot \text{Cov}(A, b) \frac{\partial\sigma_{BBC}}{\partial A} \frac{\partial\sigma_{BBC}}{\partial b} \Delta A \Delta b \end{aligned}$$

$$+ \left(\frac{\partial\sigma_{BBC}}{\partial \rho}\right)^2(\Delta\rho)^2. \quad (8)$$

The covariance(A,b) is the correlation coefficient in the two dimensional fit to the elastic slope and $dN_{el}/dt|_{t=0}$. Thus we calculate $\sigma_{BBC} = 51.15 \pm 1.60$ mb [13]. This error in σ_{BBC} of 3.1% is the main contribution to the luminosity uncertainty in run I.

4. The Number of BBC Interactions

For every beam crossing the BBC indicate either no interaction or at least one interaction. At low luminosity a positive response from the BBC counters typically indicates a single interaction, while at high luminosity on average several interactions occur during a single crossing. Thus a coincidence in the BBC indicates only that at least one interaction has occurred; we can not directly count the number of BBC interactions (N_{BBC}). An indirect method of obtaining the number of interactions is by using the formula

$$N_{BBC} = \mu N_{BC}. \quad (9)$$

Table 3
Summary of Results from Total Cross Section Measurement

		$\sqrt{s} = 1800$
N_i	Inelastic (W•E)	208890 ± 2558
N_{sd}	Inelastic (\bar{p} •E) :single diffr. (*)	32092 ± 1503
N_{el}	Elastic	78691 ± 1463
N_t	Total	319673 ± 3308
A	$dN_{el}/dt _{t=0}$ (events/GeV ²)	1336532 ± 40943
b	Elastic Slope (GeV ⁻²)	16.98 ± 0.25
Cov(A,b)	Elastic fit covariance	0.93
(*)	after removal of events triggering also (W•E)	

N_{BC} represents the number of beam crossings which is simply counted by a scaler and μ is the mean number of interactions per beam crossing. To determine the mean number of interactions we use the fact that the distribution of the number of interactions is described by a Poisson distribution with a mean μ . We can not distinguish one interaction from two or more interactions thus we will solve for the only condition that we can correctly identify that of no interactions. The Poisson probability of no interactions P_0 is related to the mean by

$$P_0 = e^{-\mu} \quad (10)$$

Solving for μ and substituting it into Eq. 9 we have

$$N_{BBC} = -(\ln P_0)N_{BC}. \quad (11)$$

This formula, which accounts for overlapping BBC interactions, is referred to as the multiple interaction correction [14].

Four scalers are used to determine P_0 . All scaler counts refer to live counts only.

- N_{BC} Number of beam crossings
- N_{EW} Number of crossings that contain a coincidence
- N_E Number of crossings that contain a hit in the east beam counters
- N_W Number of crossings that contain a hit in the west beam counters

The number of east, west, and east-west counts are converted to probabilities by normalizing to the total number of beam crossings. We relate these probabilities to physics processes as follows:

- A = processes producing an east hit with probability P_A .
- B = processes producing a west hit with probability P_B .
- C = processes producing a coincidence with probability P_C .

The probability of a hit in the east BBC (P_E) can be expressed as the sum of $P_A + P_C$ minus the overlap P_AP_C . Similarly we can express the probability of a hit in the west BBC (P_W) and the probability of a coincidence in the east and west (P_{EW}).

$$P_E = P_C + P_A - P_AP_C \quad (12)$$

$$P_W = P_C + P_B - P_BP_C \quad (13)$$

$$P_{EW} = P_C + P_AP_B - P_AP_BP_C. \quad (14)$$

Solving for P_C in terms of the scalers yields the accidental correction on the coincidence rate

$$P_C = \frac{P_{EW} - P_EP_W}{1 + P_{EW} - P_E - P_W}. \quad (15)$$

Under the assumption that the only cause of true coincidences is beam beam collisions, the probability for no interactions is produced ($P_0 = 1 - P_C$) thus yielding the number of BBC interactions [15]

$$N_{BBC} = N_{BC} *$$

$$-\ln\left(1 - \frac{N_{EW} - \frac{N_E N_W}{N_{BC}}}{(N_{BC} + N_{EW} - N_E - N_W)}\right). \quad (16)$$

5. The multiple interaction formula

During all collider running periods after 1987 [16] the bunches were separated by $3.5 \mu\text{sec}$ ($f = 286.272 \text{ KHz}$). The average luminosity for run Ib was $9.1 \times 10^{30} \text{ cm}^{-2}\text{sec}^{-1}$ and the highest luminosity was about $27 \times 10^{30} \text{ cm}^{-2}\text{sec}^{-1}$. The mean number of interactions per crossing is

$$\mu = \frac{\sigma_{BBC} \cdot L}{f} \quad (17)$$

where L is the instantaneous luminosity. The probability of at least one interaction is

$$1 - e^{-\mu} \quad (18)$$

So the number of interactions that occur is

$$M_{BBC} = (1 - e^{-\mu})N_{BC} = \frac{(1 - e^{-\mu})}{\mu}N_{BBC} \quad (19)$$

Fig. 1 shows the ratio of the number of BBC interactions to the number of BBC coincidences. This formula is known as the multiple interaction correction equation. For example at our average luminosity $9.1 \times 10^{30} \text{ cm}^{-2}\text{sec}^{-1}$, $\mu = 1.63$ and $\frac{\mu}{1 - e^{-\mu}} = 2.02$. Thus the multiple interaction correction is about 200%.

6. Details of the Luminosity Calculation

For a given Tevatron store the luminosity usually decreases as a function of time. In run Ib under good conditions the beam intensity drops by a factor of two in ten hours. Typically we calculate the luminosity many times during a given run. For run Ib we performed this calculation about 1000 times during a long store (~ 20 hours). The luminosity calculation is done every time the number of level 2 triggers has incremented by 500. The luminosity is not the same for the six bunches. With these considerations in mind, the algorithm for obtaining the luminosity is

$$L = \sum_{\text{runs}} \sum_{\text{bunches}}^6 \sum_i^{NLV2T_i} L_i \quad (20)$$

where L is the luminosity given by Eq. 2 and $NLV2T$ is the number of level 2 triggers divided by 500.

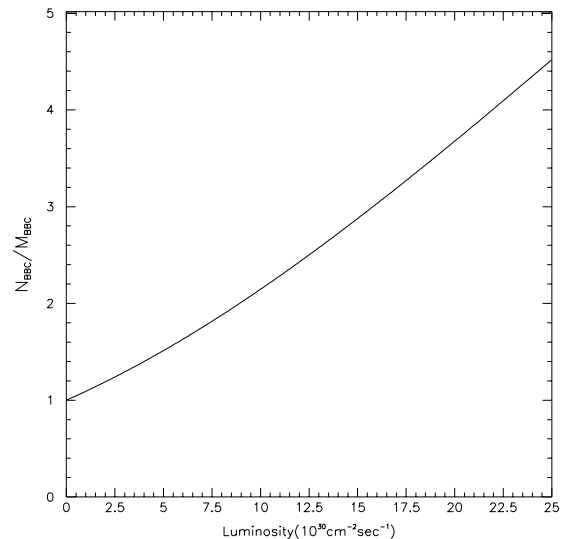


Figure 1. This plot show the multiple interaction correction as a function of luminosity. The vertical axis is the ratio of the number of BBC interactions (N_{BBC}) to the number of BBC coincidences (M_{BBC}).

When using the above formula we have implemented the following two procedures. As the data was produced by the level 3 trigger, the event order written to disk was not the original order. We have sorted the events from the beginning of the run. In addition we have forced the last event to be written to disk.

We summed over all good runs. We have removed test runs and non-physics runs from the sum. A good run requires that all run conditions such as high voltage, temperatures, currents, and fields were near the nominal value and that beam conditions were good.

7. Uncertainty in the Luminosity Calculation for run Ia

The total uncertainty on the luminosity for run Ia is 3.6%. This error is dominated by the uncertainty on σ_{BBC} (1800) which is $\pm 3.1\%$. The systematic errors are listed in Table 4.

Table 4
Luminosity errors for run Ia and Ib

Uncertainty	run Ia (%)	run Ib (%)
Measurement σ_{BBC}	3.1	3.1
Event Definition	0.5	0.5
Beam Pipe	1.0	1.0
Accidental Correction	1.0	0.0
Correlated Backgrounds	1.0	1.0
Instantaneous Luminosity	0.0	2.3
Run-to-run	0.0	0.4
Total	3.6	4.1

The ‘‘Event Definition’’ error relates to the fact that for the σ_{tot} measurement on which σ_{BBC} is based used slightly different requirements (e.g. only one of the two phototubes on each scintillator needed to be above threshold rather than both, see Ref.[13]). Between the 88-89 run and run Ia the beam pipe was reduced in thickness. Calculations show that the BBC cross section should be changed only very slightly. During run Ia the accidental correction (Eq. 11) was calculated by a procedure that is not quite correct when the luminosity varies. This leads to a small underestimate which varies with the luminosity. A correction is then applied based on the average luminosity for the file. We estimate that after this correction there is a $\pm 1\%$ error in the luminosity due to the accidental correction. The calculation for run Ib applies the formula each time the luminosity is read out, thus no systematic error is associated with the accidental correction. An estimate of the systematic shift due to other background process which produce true coincidences (e.g. beam gas interactions) has been made by taking a run with a missing bunch. The uncertainty from other backgrounds is estimated to be $\pm 0.3\%$.

8. A Consistency Check using $W \rightarrow e\nu$ Decays

To test if Eq. 16 is valid at high luminosity, we have studied the $W \rightarrow e\nu$ decay. This decay is easily identified and the selection efficiencies are well understood. This cross section has been mea-

sured by the CDF collaboration and is $\sigma_{\text{B}}(W \rightarrow e\nu) = 2.49 \pm 0.02$ (stat) ± 0.08 (syst) ± 0.09 (lum) [13]. The W selection is essentially the same as our earlier analysis, except that we have increased the \cancel{E}_{T} cut from 20 GeV to 30 GeV. Table 5 shows the number of $W \rightarrow e\nu$ candidates where the run Ia data is now analyzed using the same cuts as the run Ib data.

Table 5
Number of $W \rightarrow e\nu$ Candidates for run I

Run	W Candidates	Luminosity (pb^{-1})
Ia	9690 ± 98	19.65
Ib	41563 ± 204	86.47

However, we must correct the data for small differences in efficiency and background.

8.1. Trigger

The trigger efficiencies do not differ significantly between run Ia and run Ib.

8.2. Acceptance

The dominant effect on the acceptance is the smearing of the missing transverse energy (\cancel{E}_{T}) due to the extra-interaction energy. Our analysis uses a \cancel{E}_{T} cut of 30 GeV which is robust to smearing. We have run a Monte Carlo simulation where extra-interaction energy from minimum-bias data is included with the W simulation. When the luminosity weighted results for run Ia and Ib are compared no difference is seen.

8.3. ID efficiency

The ID efficiency is the efficiency for the electron to pass all the quality cuts imposed for W electron identification. It is known that the variables used in the selection degrade with more interactions per crossing. For example, extra interaction energy deposited near an electron can spoil the electron isolation. We have studied this using $Z \rightarrow e^+e^-$ events. The Z 's are identified without imposing quality cuts on the second electron. The correction to the number of events ($N_{\text{Ib}}/N_{\text{Ia}}$) due to ID efficiency is 1.005 ± 0.015 , dominated

by the statistical uncertainty in the run Ia $Z \rightarrow e^+e^-$ data sample.

8.4. Overlap between Leptons and Jets

The lepton-jet efficiency accounts for the requirement that the electron be separated from jets by 1.3 times the cone clustering size. This is helpful because a small number of electrons are not reconstructed due to complete electron-jet overlap.

We measure the electron-jet separation efficiency by re-decaying Z bosons many times and looking at the probability of the electron falling near a jet. The procedure is applied to both run Ia and Ib. The correction to the number of events (N_{Ib}/N_{Ia}) is 1.004 ± 0.001 .

8.5. Vertex

Our W selection includes the requirement that the event vertex be within 60 cm of the center of the detector. Fig. 2 shows the z distributions for $W \rightarrow e\nu$ data.

The fits show a wider z distribution for run Ib than for run Ia. The correction to the number of events (N_{Ib}/N_{Ia}) is 1.009 ± 0.010 .

8.6. QCD Background

The QCD background is defined as multi-jet events in which a jet passes electron selection criteria and the transverse energy is mis-measured to the extent that the event passes the \cancel{E}_T cut. The QCD background increases as the luminosity increases. This occurs because the extra interactions cause our \cancel{E}_T resolution to be degraded and the fraction of multi-jet events in the sample to be increased. The QCD background has been carefully analyzed. The main source of background is multijet contamination. Multijet contamination is measured with a sample obtained by removing the electron isolation and neutrino requirements of the W selection and then extrapolating from the multijet-dominated region into the W signal region. These extrapolations have been applied to run Ia and Ib and show that $N_{Ib}/N_{Ia} = 0.985 \pm 0.006$. These results have been checked by using LO QCD(VECBOS) with partial higher order corrections via HERWIG to model $W \rightarrow e\nu$. The detector responses were modeled using a simulation of the CDF detector. The modeling was

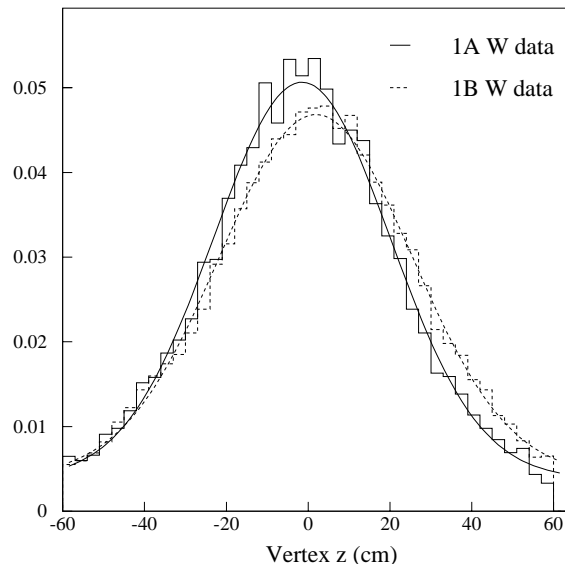


Figure 2. The z distribution for vertices in the $W \rightarrow e\nu$ data. The solid line is a fit to the run Ia data ($\sigma = 25.4$ cm) and the dashed line is a fit to the run Ib data ($\sigma = 26.5$ cm).

improved by adding the effects of the additional interaction energy into the degradation of \cancel{E}_T resolution.

8.7. Other Backgrounds

Other backgrounds to the $W \rightarrow e\nu$ data sample include $W^\pm \rightarrow \tau^\pm\nu$, $Z \rightarrow e^+e^-$, and $Z \rightarrow \tau^+\tau^-$. These backgrounds are measured using Monte Carlo simulations. There are no parameters in the calculation that differ between run Ia and Ib. The corrections are small in magnitude and we do not expect a significant dependence on instantaneous luminosity. We assign a relative correction of 1.0 to the run Ib to Ia ratio.

8.8. Conclusion

The corrections to the number of W 's are small and are given in Table 6.

The luminosity we expect for run Ib based on

Table 6
Corrections to $\frac{N_{Ib}}{N_{Ia}}$

Correction	Ratio
C_{Trigger}	1.000 ± 0.004
$C_{\text{Acceptance}}$	1.000
C_{ID}	1.005 ± 0.015
$C_{\text{lepton-jet}}$	1.004 ± 0.001
C_{vertex}	1.009 ± 0.010
C_{QCD}	0.985 ± 0.006
$C_{\text{Other Backgrounds}}$	1.0 ± 0.000
$C_{\text{correction}}$	1.002 ± 0.016

the number of W 's detected is

$$\begin{aligned} L_{\text{expected Ib}} &= C_{\text{correction}} \left(\frac{N_{Ib}}{N_{Ia}} \right) L_{Ia} \\ &= 84.45 \pm 2.05 \text{ pb}^{-1} \end{aligned} \quad (21)$$

The error includes the W counting errors, the portion of the luminosity error specific to run Ia, and the error on the relative correction factor. We see that the expected result is consistent with our measured value of $L = 86.5 \pm 3.5 \text{ pb}^{-1}$ (see Tables 4 and 5).

9. Run to Run Variation in the W cross section for run Ib

Fig. 3 shows the $W \rightarrow e\nu$ rates versus instantaneous luminosity for our run Ib data. The figure shows that the rate drops with increasing instantaneous luminosity and that the rate matches the run Ia value in the low instantaneous region. If we assume that the drop is due to an over measurement of integrated luminosity at high instantaneous luminosity than we can apply a correction to flatten the plot. Although the correction can be as large as 10% at the highest instantaneous luminosities the overall shift is 2-3 percent. This is simply because most of our data is collected at luminosities where the offset from run Ia is small.

Fig. 4 shows the $W \rightarrow e\nu$ run Ib rates versus run number. The rates are stable to better than 5%. A possible deficit is noticeable at the end of the run. This decrease is consistent with the above hypothesis as the average instantaneous luminosity was larger near the end of the run.

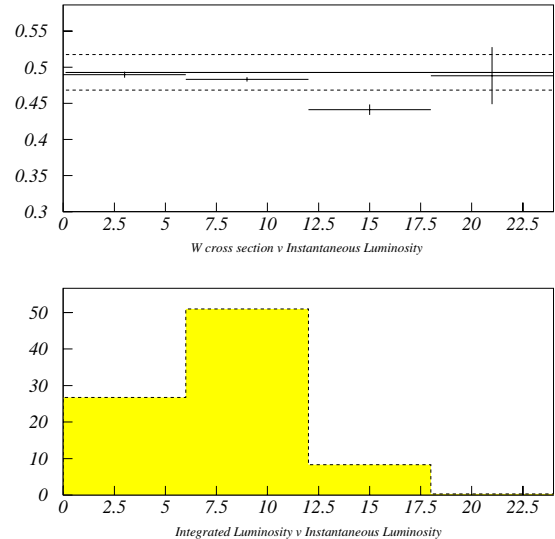


Figure 3. The $W \rightarrow e\nu$ rates (N_W/L) versus instantaneous luminosity (upper) plot and the integrated luminosity (pb^{-1}) for each instantaneous luminosity bin (lower). The horizontal lines represent the run Ia value $\pm 5\%$ variations.

Fig. 5 shows the $W \rightarrow e\nu$ rates per run for the 1030 runs from run Ib. The run-to-run scatter is consistent with the $W \rightarrow e\nu$ counting uncertainty. This is evident from the χ^2 plot shown in the lower part of the figure. We should note that any source of run-to-run fluctuation in the luminosity calculation due to changing beam conditions or BBC hardware problems might not be large enough to show in this plot. One way to determine the maximum size of any possible additional fluctuations is to add in quadrature an extra term to the counting error. We increase this contribution until the probability distribution is inconsistent with a flat distribution at the 95% confidence level. This is illustrated in Fig. 6. Using this procedure we assign a 7% uncertainty to the integrated luminosity on a run-by-run basis. When this error is propagated through the total luminosity in run Ib the uncertainty is 0.36%.

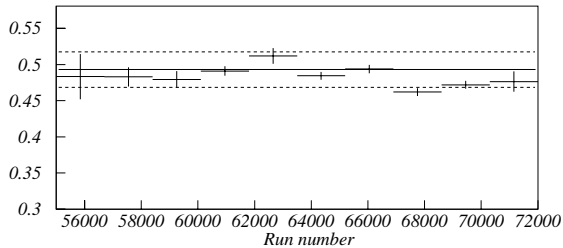


Figure 4. The $W \rightarrow e\nu$ rates (N_W/L) versus run number. No background subtraction or efficiency applied. The horizontal lines represent the run Ia value with $\pm 5\%$ variations.

10. Uncertainty in the luminosity calculation for run Ib

The total uncertainty on the luminosity for run Ib is 4.1%. Again, as in run Ia, the error is dominated by the uncertainty on $\sigma_{\text{BBC}}(1800)$ which is 3.1%. The systematic errors are listed in Table 3. The event definition and beam pipe errors are also the same as for run Ia. As indicated in section 7 we now have no systematic error associated with the accidental correction. In section 8 we checked the stability of the luminosity calculation across run Ia and Ib, and during run Ib as a function of instantaneous luminosity. The rates are seen to drop with increasing instantaneous luminosity from the run Ia value at low luminosity. After correcting for efficiencies and backgrounds that differ between run Ia and run Ib we find that the W yields were consistent at the 2.34% level. We have decided to include this value as a systematic uncertainty due to changes in the measurement of the luminosity as a function of instantaneous luminosity. The run-to-run fluctuations in run Ib give rise to a 0.36% uncertainty in the luminosity. The systematic errors are listed in Table 4.

11. Vertex Reconstruction

This section describes a cross check on the BBC measured luminosity. The average number of in-

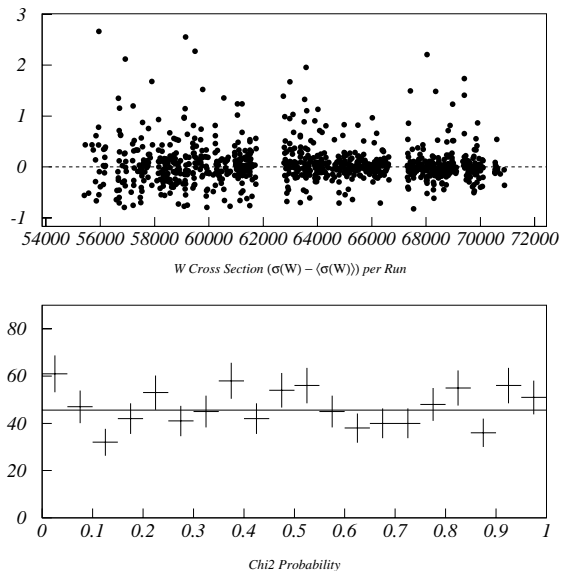


Figure 5. The upper plot shows the $W \rightarrow e\nu$ cross sections (with no corrections applied) minus the mean value for all runs in our run Ib data sample. The lower plot shows the probability χ^2 distribution. The only uncertainty used in the χ^2 calculation is the counting error on the $W \rightarrow e\nu$ candidates.

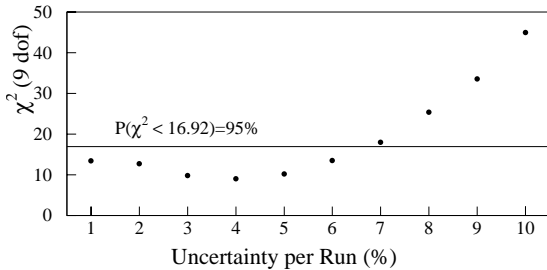


Figure 6. The χ^2 of the fit of a flat line to Fig. 5 after adding an additional error for luminosity. The horizontal axis is the uncertainty of luminosity per run. When this value is larger than 7% the Probability χ^2 distribution is inconsistent with a flat line indicating the error is too large.

teractions in a $p\bar{p}$ crossing depends on the instantaneous luminosity. Although we can not count the number of interactions in a particular crossing we can use the vertex detector (VTX) to count the number of vertices [17]. The VTX is a vertex time-projection chamber used for vertex finding. The number of well reconstructed vertices at a particular instantaneous luminosity can then be compared to the predictions for a given instantaneous luminosity provided the vertex reconstruction efficiency is known.

The actual observable we use is the ratio (R) of number of events with one or more vertices to the number of events with no vertices. This ratio will increase as the instantaneous luminosity increases. We will show that if the BBC are performing accurately at low luminosity then we can check for consistency between the BBC and the VTX at high instantaneous luminosity.

We use two data samples: a min-bias sample which is triggered on a BBC coincidence and our standard W sample. Fig. 7 shows the ratio of events with at least one well reconstructed vertex to those with no well reconstructed vertices for the min-bias sample. Fig. 8 shows the same distribution for the W sample. Since the reconstruction efficiency of a W boson vertex is not necessarily the same as that for a generic vertex

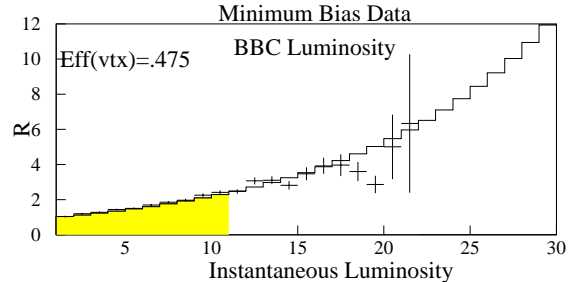


Figure 7. The ratio (R) of the number of events with one or more well reconstructed vertices to the number with 0 well reconstructed vertices in the minimum bias data sample. The horizontal axis is instantaneous luminosity in units of $10^{30} \text{ cm}^{-2} \text{ sec}^{-1}$. The line represents the prediction at the given luminosity. The data points are measured values of R placed at the instantaneous luminosity measured by the BBC.

we only count vertices in addition to the W boson vertex. The vertex reconstruction efficiency used in Fig. 7 and 8 has been chosen to give good agreement between the measured value of R and that predicted by the equations in this section for the lower portion of the curve (shaded region). This vertex efficiency is essentially identical with an independent determination used in our “Double Parton” analysis [18].

The predictions for R are obtained by generating a Poisson distribution of BBC interactions with a mean μ (Eq. 17) and folding in the vertex efficiency. In terms of probability R can be expressed as

$$R = \frac{P_{\geq 1}}{P_{=0}} \quad (22)$$

where $P_{\geq 1}$ represents the probability for reconstructing one or more high quality vertices. $P_{\geq 1}$ is calculated from the probability of reconstructing m high quality vertices given n interactions. The value depends on the efficiency of reconstructing the vertex, ϵ , the number of ways one can choose m vertices from the n interactions and

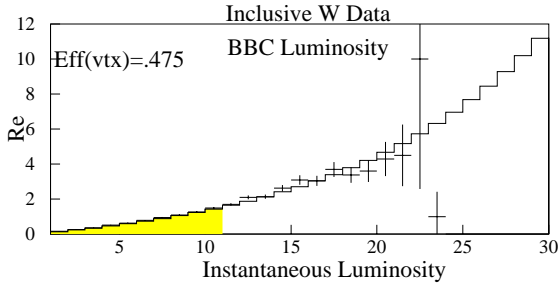


Figure 8. The ratio (R_e) of the number of events with one or more well reconstructed vertices to the number with 0 well reconstructed vertices in the $W \rightarrow e\nu$ data sample. The horizontal axis is instantaneous luminosity. The line represents the prediction at the given luminosity in units of $10^{30} \text{ cm}^{-2} \text{ sec}^{-1}$. The data points are measured values of R_e placed at the instantaneous luminosity measured by the BBC.

the probability of getting n interactions

$$P_{\geq 1} = \sum_{n=m}^{\infty} \sum_{m=1}^{\infty} \left(\frac{n!}{m! \cdot (n-m)!} \cdot \epsilon^m \cdot (1-\epsilon)^{(n-m)} \cdot \frac{\mu^n e^{-\mu}}{n!} \right). \quad (23)$$

We start with a minimum value of one for m because we need at least one vertex. The sum over interactions (n) for each vertex multiplicity starts with a minimum value of m . The denominator of R is calculated by considering the probability of having n interactions and failing to reconstruct a high quality vertex for every interaction

$$P_{=0} = \sum_{n=1}^{\infty} (1-\epsilon)^n \frac{\mu^n e^{-\mu}}{n!}. \quad (24)$$

Note the $P_{=0} + P_{\geq 1}$ does not sum to one. This is because we have not included any terms with zero interactions. Our data sample for the min-bias trigger requires events to have at least one interaction because of the BBC trigger requirement.

We now proceed to calculate the ratio R_e in the $W \rightarrow e\nu$ sample. For a given luminosity there are on average μ interactions so there are on average

μ ways of selecting the W interaction, and we need to multiply the equations by μ . We must also remove the W vertex from our combinatorial factor ($n \rightarrow (n-1)$). Thus the corresponding formula for reconstructing vertices in $W \rightarrow e\nu$ events are:

$$R_e = \frac{P_{\geq 1}(e)}{P_{=0}(e)} \quad (25)$$

$$P_{\geq 1}(e) = \sum_{n=m}^{\infty} \sum_{m=1}^{\infty} \left(\frac{(n-1)!}{m! \cdot ((n-1)-m)!} \cdot \epsilon^m \cdot (1-\epsilon)^{((n-1)-m)} \cdot \frac{\mu^n e^{-\mu}}{(n-1)!} \right) \quad (26)$$

$$P_{=0}(e) = \sum_{n=1}^{\infty} (1-\epsilon)^{n-1} \cdot \frac{\mu^n e^{-\mu}}{(n-1)!}. \quad (27)$$

Our predictions for R and R_e are overlaid with the data in Fig. 7 and Fig. 8. The theory shows what one should measure for R at a particular luminosity. In Fig. 7 we see that R approaches ≈ 1.0 at the lowest luminosity. Every event in the min-bias sample has at least one BBC interaction because of the trigger requirement. At the lowest luminosity the min-bias sample will be dominated by events with one and only one interaction. If half of these interactions are reconstructed with the highest quality vertex, then the number of events with one or more vertices equals the number of events with no reconstructed vertices. Therefore in the limit of low luminosity we can read off the vertex reconstruction efficiency. This efficiency includes the efficiency for the vertex to be within 60 cm of the center of the detector. The efficiency used in the prediction is varied until the data in the low luminosity region is reproduced. Both R and R_e show good agreement with the BBC luminosity in the high luminosity region.

12. Luminosity for all triggers

In a complex experiment like CDF there are very many triggers. The most important triggers for the analysis of top quarks or the W mass were not prescaled. However, because of limits in level

3 processor power, many triggers were prescaled. The prescale factor may be fixed or dynamic (a function of the luminosity). The prescale factor is the ratio of the number of events that pass a trigger before and after prescaling is applied. The prescale luminosity is calculated at each increment of 500 level 2 triggers (see Section 6). The luminosity for a given trigger T is obtained by summing over all increments during a run

$$L_T = \sum_{i=1} p_i L_i. \quad (28)$$

Fig. 9 shows the prescale factor as a function of run number and also versus a run's integrated luminosity for a jet trigger.

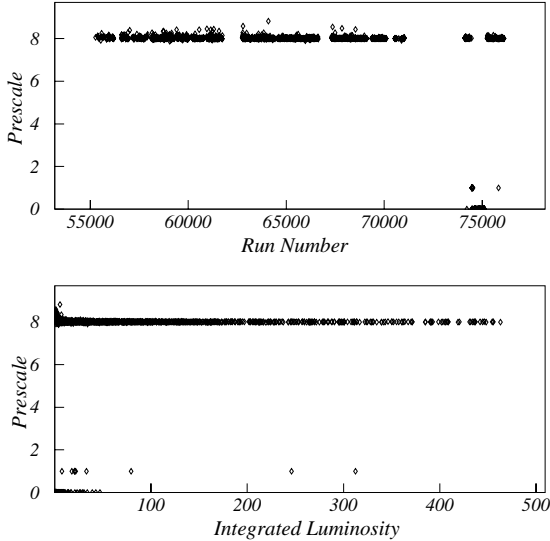


Figure 9. The ratio of unprescaled luminosity for the Jet₇₀ trigger. The upper plot shows the value versus run number and the lower plot shows the value versus a run's integrated luminosity in nb^{-1} .

As we can see the prescale is 8 for most runs. The scatter in the plots is due to the statistics of low integrated luminosity runs. The runs with prescale factor of zero were taken during a

short 630 GeV running period. As can be seen a few runs were taken with a prescale factor of one. Fig. 10 shows the instantaneous luminosity versus event number (top) and the prescale factor versus event number (bottom) for a forward electron + \cancel{E}_T trigger. For this particular run

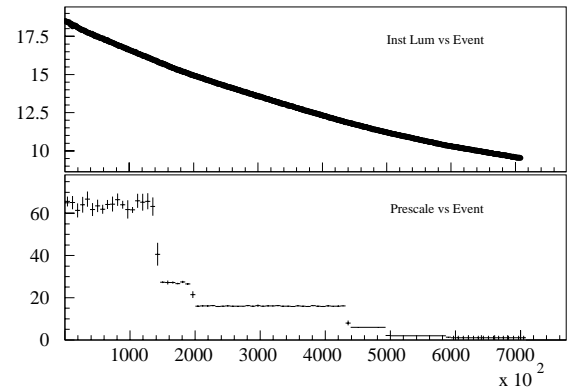


Figure 10. The top plot shows the instantaneous luminosity ($10^{30} \text{ cm}^{-2} \text{ sec}^{-1}$) versus event number for run 69808. The lower plot shows the measured prescale versus event number for the forward electron + missing E_T trigger.

(#69808) the prescale is set initially to 64 and drops until at the end of the run it is 1. With the above algorithm, we have provided the integrated luminosity for all 267 level 2 triggers.

13. Conclusions

The beam-beam counters have yielded a measurement of the luminosity with an error of 3.6% for run Ia and 4.1% for run Ib. It is important to note that this measurement and all corresponding cross section measurements depend on our earlier measurement of the total cross section. CDF uses only our own cross section measurement as the BBC cross section is proportional to the total cross section (Eq. 3), and the denominator of the proportional factor $\frac{N_{\text{BBC}}}{N_{\text{inel}} + N_{\text{el}}}$ is also taken from our cross section measurement. The consistency

of the $W \rightarrow e\nu$ rates as a function of luminosity and run number give us confidence in our result. We have also checked the results by comparing the number of events with one or more vertex to the number with no vertices. For run I, the total integrated luminosity for a typical data set ($W \rightarrow e\nu$) is $106.1 \pm 4.1 \text{ pb}^{-1}$. Finally we indicate how we obtained the luminosity for all triggers taken during run Ib.

Acknowledgments

Although many people contributed to the CDF measurement of the luminosity we would like to especially thank members of the University of Chicago group who designed, built and maintained the beam-beam counters and also provided the software for run Ia, M. Campbell, M. Contreras, H. Frisch, C. Grosso-Pilcher, S. Kopp, T.M. Liss, G. Redlinger and J. Wang. We also thank S. Belforte, M. Binkley, K. Burkett, A. Byon-Wagner, M. Dell'Orso, J.E. Elias, A.T. Goshaw, K. Goulios, H. Jensen, J.D. Lewis, J.P. Marriner, L. Nodulman, A. Nomerotski, M.P. Schmidt, S. Segler, and S. Tkaczyk for their help in this work. We would also like to thank R. Herber for help with PostScript.

REFERENCES

1. F. Abe *et al.*, Nucl. Instrum. Methods Phys. Res., Sect. A **271**, (1988) 387.
2. D. Amidei *et al.*, Nucl. Instrum. Methods Phys. Res., Sect. A **269**, (1988) 51.
3. V. Bharadwaj, J. Crawford, R. Mau, in Proceedings of the 1995 Particle Accelerator Conference and International Conference on High-Energy Accelerators, IEEE, Dallas (May 1995) 443.
4. John Marriner, in Proceedings of the 10th Topical Workshop on Proton-Antiproton Collider Physics, Batavia Illinois, 1995, edited by R. Raja and J. Yoh (AIP Press) 189.
5. F. Abe *et al.*, Phys. Rev. Lett. **62**, (1989) 613.
6. M. Bozzo *et al.*, Phys. Lett. **147B**, (1984) 392.
7. G.J. Alner *et al.*, Z. Phys. C **32**, (1986) 152.
8. F. Abe *et al.*, Phys. Rev. D **44**, (1991) 29.
9. F. Abe *et al.*, Phys. Rev. D **50**, (1994) 5518.
10. F. Abe *et al.*, Phys. Rev. D **50**, (1994) 5535.
11. F. Abe *et al.*, Phys. Rev. D **50**, (1994) 5550.
12. N. Amos *et al.*, Phys. Rev. Lett. **68**, (1992) 2433.
13. F. Abe *et al.* Phys. Rev. Lett. **76**, (1996) 3070.
14. Hans Jensen developed this correction.
15. M. Dell'Orso, private communication.
16. During the 1987 run the bunches were separated by 7μ sec.
17. F. Snider *et al.*, Nucl. Inst. and Methods, **A268**, (1988) 75. This is the reference for the previous generation of the device. The replacement for run I has more modules, each with a shorter drift length.
18. F. Abe *et al.* Phys. Rev. D **56**, (1997) 3811.